

cally with λ . The variation of $P_2/(P_2)_{\lambda=0}$ with η_2 and λ is illustrated in Fig. 1 for typical values of γ , K , and ξ_1 .

The variation of duct length with λ is more complicated. If $L(\eta_2; \lambda)$ is the generator length for an output $H_1(1 - \eta_2)$ per unit of mass flow, then from (9)

$$\frac{\partial L}{\partial \lambda} = \frac{(H_1/2)^{1/2} \rho_1}{K(1-K)B^2 \sigma_1} \int_{\eta=\eta_2}^1 g \frac{\partial}{\partial \lambda} (\ln g) d\eta$$

$$\frac{(1+z)(1-K)}{K(1-\lambda)^2(1-\eta)} \left(\frac{\partial \beta}{\partial \lambda} \right)^{-1} \frac{\partial}{\partial \lambda} (\ln g) =$$

$$\frac{\gamma-1}{2\gamma\{\xi_1 - \lambda(1-\eta)\}} + \frac{1}{\gamma} \left\{ \frac{\gamma(1+z) - (\gamma-1)(1+y)}{(\eta-\xi_1) + \lambda(1-\eta)} \right\} +$$

$$\frac{(1+z)(1-K)}{K(1-\lambda)^2(1-\eta)} f(\eta; \lambda) \quad (10)$$

Now $g > 0$; $f > 0$; $\partial \beta / \partial \lambda > 0$ for all η, λ , so that $\text{sgn}(\partial L / \partial \lambda)$ is given by the sign of the right side of Eq. (10) in which only the second term can be negative. Note that $\partial(\ln g) / \partial \lambda = 0$ for $\eta = 1$. Clearly, for y less than, or slightly greater than, $(z\gamma + 1)/(\gamma - 1)$, the generator length increases monotonically with increasing λ for all permissible values of the parameters. For large values of y , the second term of Eq. (9) is negative and becomes the dominant term as η decreases from 1 to η_2 .

Closed Cycle Power Generation

The conclusions reached previously may be stated as follows: The value of λ determines what fractions of the total power are extracted at the expense of kinetic energy and of static enthalpy. For $\lambda = 0$, energy is extracted from the static enthalpy only; when $\lambda = 1$ power is taken from the kinetic energy only. For a given total power per unit mass flow, the loss of stagnation pressure decreases as λ increases. When the temperature dependence of conductivity is weak, the generator length increases as λ increases. For strong temperature dependence, this effect is reversed.

These results are, of course, not surprising, and could be deduced from physical considerations or from an examination of the initial equations. What they are intended to illustrate here is the usefulness of the parameter λ in defining generator operation. There is no reason why one should be restricted to constant velocity, temperature, etc., as seems to have been the case hitherto. Analyses of closed cycle MHD-turbine generating plants, such as those of Gunson et al.,³ or of Sodha and Bendor,⁴ are usually carried out for constant velocity or constant Mach number when, in fact, the selection of a somewhat higher value of λ would have led to a reduction in both the generator length and the pressure drop.

The generator dimensions enter the efficiency estimation of a closed cycle system through the heat lost from the duct and the power required to produce the magnetic field. These are given by the integral over the generator length of the product of the temperature difference between gas and duct walls and some transverse dimension of the duct. Expression could be written down for the heat loss (as in Sodha and Bendor⁴ for constant M only), and their variation with λ examined. It can also be shown that the duct dimensions at exit increase with increasing λ for given entry conditions and η_2 . Thus, for weak temperature dependence of conductivity, the heat loss increases more rapidly with λ than the generator length. For a rapidly varying conductivity, one may expect the positive variation of closed cycle efficiency with λ , resulting in this case both from a reduction in pressure loss and in generator length, to be reduced, and for high values of λ , even reversed.

References

- 1 Sutton, G. W., "The theory of magnetohydrodynamic power generators," General Electric Space Sciences Lab., Rept. R62SD990, pp. 112-140 (December 1962).

² Swift-Hook, D. T. and Wright, J. K., "The constant Mach number MHD generator," J. Fluid Mech. 15, 97-110 (January 1963).

³ Gunson, W. E., Smith, E. E., Tsu, T. C., and Wright, J. H., "MHD power conversion," Nucleonics 21, 43-47 (July 1963).

⁴ Sodha, M. S. and Bendor, E., "Enhancement of gas conductivity by dust suspension and its application to closed cycle magnetohydrodynamic power generation," Brit. J. Appl. Phys. 15, 1031-1040 (1964).

Radial Lag of Solid Particles in Delaval Nozzles

E. DOUGHMAN* AND C. H. LEWIS JR.†

Philco Research Laboratories, Newport Beach, Calif.

RECENTLY a light scattering technique has been used to study particle trajectories in nozzle plume gas-particle flows. In this note, experimental measurements of the radial spreading of the particle cloud are compared with results calculated by a computer program developed to determine solid particle velocity and thermal lags in rocket nozzles.¹ The particle spreading at the nozzle exit is compared with theory for both large (glass beads) and small (alumina) particles. The observed particle boundary was found to compare well with the theoretical limiting particle streamline† for the small size particles from each powder size distribution.

The experimental facility consisted of a 3800 ft³ blow-down vacuum tank through which a mixture of nitrogen gas and solid particles could be fed and studied with appropriate instrumentation. The mixing of the particles and the gas was accomplished by forcing the particles into the gas stream with a piston driven by gas pressure. In addition to light scattering photography, instrumentation included measurements of stagnation, exit plane, and tank pressures and gas and particle flow rates. A conical nozzle was used

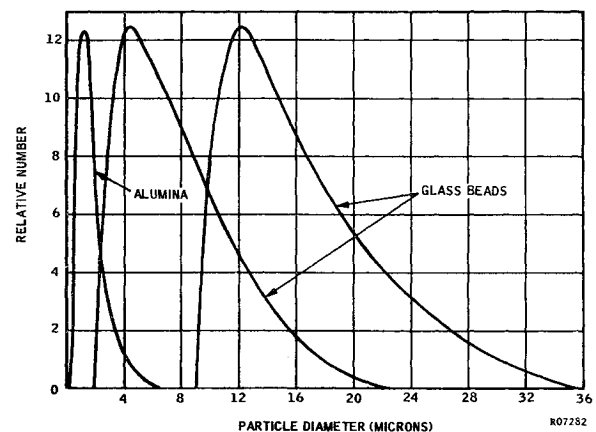


Fig. 1 Particle size distributions.

Received July 30, 1964. This research is part of Project DEFENDER under joint sponsorship of the Advanced Research Projects Agency, Department of Defense, and the Office of Naval Research. The work described herein was performed under Contract No. NOnr 3907(00), ARPA Order 237-62, Amendment No. 7.

* Research and Development Engineer, Fluid Mechanics Department. Associate Member AIAA.

† Research and Development Engineer, Propulsion Department. Member AIAA.

‡ The "limiting streamline" for a given size particle is defined as that particle trajectory that passes closest to the nozzle wall without impingement.

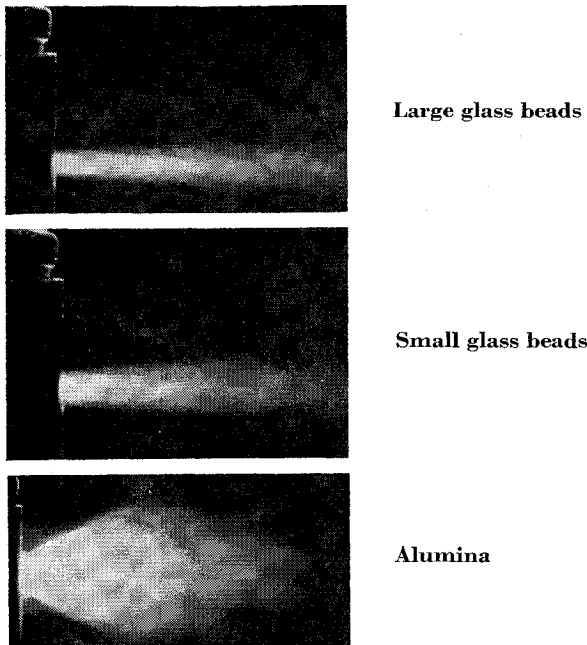


Fig. 2 Photographs of scattered light from particle plumes.

with a throat diameter of 0.260 in. and an expansion cone half-angle of 15° with an area ratio of 3.87.

The theoretical calculations show that particle trajectories depend upon the initial position of the particle, the nozzle contour (especially the subsonic convergent portion), gas stagnation pressure, and particle size and specific gravity. As the particle size decreases, the particle plume boundary for that size moves further from the plume axis; that is, the size-dependent limiting streamlines subtend a greater included angle. Thus, for a given size distribution, the outer boundary should be formed by the smaller size particles. In order to compare theory with experiment, a light scattering technique was employed. A two-dimensional sheet of visible light was passed through a cold gas-particle plume so that the plume axis lay in the plane of the light beam. Photographs of the light scattered in a direction normal to the sheet were taken to visualize the plume. The quantity of light scattered from a volume element depends upon the concentration of scatters there, so that regions of high particle concentration appear brighter in the photographic image.

Three powders with different minimum sizes were used to show the effect of particle size. Two size distributions were of glass beads, approximately 90% spheres, and one of alumina (see Fig. 1). From photographs taken with the electron microscope, the smallest alumina particle was found to be roughly 0.25μ in radius with the most abundant size at about 0.8μ . In contrast, the smallest glass particles for the two size distributions were about 1.0 and 5.0μ , respec-

Table 1 Comparison of experiment and theory for particles with radii corresponding to the lower limit of the size distribution

	Minimum particle radius, μ	$\left(\frac{D}{D_{\text{exit}}}\right)_{\text{expt}}$	$\left(\frac{D}{D_{\text{exit}}}\right)_{\text{theo}}$
Glass beads	5	0.4	0.40
Glass beads	1	0.6	0.62
Alumina	$\frac{1}{4}$	1.0	0.85

tively. Photographs of the scattered light are shown in Fig. 2. In each case, the chamber pressure was 100 psig, exit pressure 200 mm Hg, tank pressure 4 mm Hg, and the particle mass flow rate to gas flow rate ratio was 0.3. The computer program was used to determine the limiting streamline radial location at the exit plane of the nozzle as a function of particle size as shown in Fig. 3. The diameter of the particle plume at the exit plane D , as obtained from the photographs, was compared with the diameter calculated for the limiting streamlines for the minimum particle size in each distribution. The good agreement between experiment and theory, shown in Table 1, is taken as a demonstration of the validity of the theory.

Reference

¹ Carlson, D. J., "Measurement of velocity lag of condensed phases in gas-particle nozzle flows," AIAA J. (submitted for publication).

Effect of Azimuth on the Accuracy of an Interferometer Radar

C. W. PITTMAN*

Aerospace Corporation, Los Angeles, Calif.

Introduction

AN interferometer radar measures the position and/or velocity of a target by determining the range and/or range rate of the target from a number of tracking stations simultaneously. At least three measurements are required. A coordinate transformation to polar or rectangular coordinates is then performed by a calculation that is geometrically equivalent to finding the point of intersection of three spheres. The angle measurements from the central station (azimuth and elevation) are found to be primarily functions of the range (or range rate) differences between the stations denoted as p and q . Errors in p and q (or \dot{p} and \dot{q}) will result in errors in A and E (or \dot{A} and \dot{E}).

The General Electric (GE) Mod III Atlas guidance system at the Eastman Test Range (ETR) uses a doppler-measuring interferometer subsystem with three ground stations in an L configuration. In the analysis that follows, it is shown that 1) the errors in \dot{p} and \dot{q} behave to a considerable extent as if they originated in three independent noise sources (i.e., each of the ground stations); and 2) if this is so, then the angular rate accuracy of the subsystem is a function of the azimuth of the target relative to the baselines between the ground stations.

Figure 1 illustrates the variation in accuracy as a function of azimuth. Note that it is assumed that the raw measurement accuracy at each of the stations does not vary with azimuth. The variation is due to the changing sensitivity of the angular rates with respect to the raw measurements.

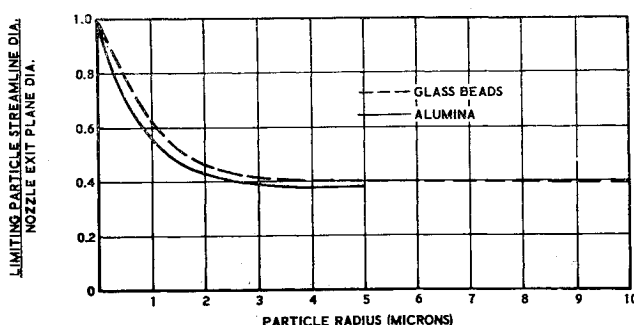


Fig. 3 Location of limiting particle streamline at the nozzle exit as a function of particle size.

Received August 3, 1964.

* Manager, Radio Analysis Section, Electronics Division.